

Lawrence Berkeley National Laboratory

Molecular Foundry

Title

Off-Cycle Processes in Pd-Catalyzed Cross-Coupling of Carboranes

Permalink

<https://escholarship.org/uc/item/2f12p28s>

Journal

Organic Process Research & Development, 23(8)

ISSN

1083-6160

Authors

Dziedzic, Rafal M
Axtell, Jonathan C
Rheingold, Arnold L
[et al.](#)

Publication Date


2019-08-16

DOI

10.1021/acs.oprd.9b00257

Peer reviewed

Off-Cycle Processes in Pd-Catalyzed Cross-Coupling of Carboranes

Rafal M. Dziejczak,[†] Jonathan C. Axtell,[†] Arnold L. Rheingold,[‡] and Alexander M. Spokoyny^{*,†,§} 

[†]Department of Chemistry and Biochemistry, University of California, Los Angeles, 607 Charles E. Young Drive East, Los Angeles, California 90095, United States

[‡]Department of Chemistry and Biochemistry, University of California, San Diego, 9500 Gilman Drive, La Jolla, California 92093, United States

[§]California NanoSystems Institute (CNSI), University of California, Los Angeles, 570 Westwood Plaza, Los Angeles, California 90095, United States

Supporting Information

ABSTRACT: Off-cycle processes in a catalytic reaction can dramatically influence the outcome of the chemical transformation and affect its yield, selectivity, rate, and product distribution. While the generation of off-cycle intermediates can complicate reaction coordinate analyses or hamper catalytic efficiency, the generation of such species may also open new routes to unique chemical products. We recently reported the Pd-mediated functionalization of carboranes with a range of O-, N-, and C-based nucleophiles. By utilizing a Pd-based catalytic system supported by a biarylphosphine ligand developed by Buchwald and co-workers, we discovered an off-cycle isomerization process (“cage-walking”) that generates four regioisomeric products from a single halogenated boron cluster isomer. Here we describe how several off-cycle processes affect the regioisomer yield and distribution during Pd-catalyzed tandem cage-walking/cross-coupling. In particular, tuning the transmetalation step in the catalytic cycle allowed us to incorporate the cage-walking process into Pd-catalyzed cross-coupling of sterically unencumbered substrates, including cyanide. This work demonstrates the feasibility of using tandem cage-walking/cross-coupling as a unique low-temperature method for producing regioisomers of monosubstituted carboranes.

KEYWORDS: *off-cycle, catalysis, carboranes, cage-walking, deboronation*

INTRODUCTION

Since the discovery of metal-catalyzed cross-coupling, researchers have observed off-cycle processes in the manipulation of hydrocarbon-based molecules (e.g., metal-mediated β -hydride elimination and chain-walking).^{1–3} While off-cycle processes may lead to catalytically inactive byproducts that hamper the efficiency of catalytic cycles,^{4,5} understanding these off-cycle processes is critical for improving the reaction selectivity and suppressing detrimental reaction pathways. Off-cycle processes in metal-catalyzed reactions can have utility as alternate reaction pathways that enable new or nonintuitive reactivity in synthesis.^{6–12}

An appealing aspect of off-cycle processes is the isomerization of a substrate molecule into regioisomers that cannot be easily synthesized.¹³ Such isomerization reactions are particularly useful when studying structure–activity relationships among isomers because these reactions can help identify lead compounds from a single reactant.¹⁴

We and others have recently been expanding the application of Pd-based cross-coupling methodology to three-dimensional (3D) icosahedral carborane substrates.^{15–27} These compounds possess several unique spectroscopic features such as NMR-active ¹¹B and ¹⁰B nuclei, IR- and Raman-active B–H bond stretching modes, and distinct ¹¹B/¹⁰B isotopic patterns in mass spectrometry, enabling detection of icosahedral boranes by a variety of analytical methods.^{28–31} In particular, the three isomers (ortho, meta, and para) of dicarba-*closo*-dodecaboranes (*o/m/p*-C₂B₁₀H₁₂) are of interest because of their commercial availability and their utility as 3D scaffolds in

molecular design. The *o*- and *m*-C₂B₁₀H₁₂ isomers both have pronounced dipole moments, four sets of chemically inequivalent B–H vertices, and one set of chemically equivalent C–H vertices. The variety of substituted regioisomers available to carboranes allows them to act as electronically distinct, isosteric functional groups (Figure 1). The electronic diversity among carborane regioisomers has enabled tuning of their hydrophobicity, pharmacological properties, photoluminescence, and surface chemistry.³²

Among the presently available boron vertex functionalization methods, metal-catalyzed transformations enable the installation of the broadest class of chemical groups. These metal-catalyzed methods can be loosely grouped into (1) directed B–H activation and (2) cross-coupling at B–X bonds (X = Br, I).^{33–35} While B–H activation methods often target the electron-deficient B–H vertices (those closest to the carbon vertices),^{36,37} cross-coupling at B–X bonds can occur at electron-rich and electron-poor boron vertices.³⁸ Thus, direct and selective synthesis of halocarborane regioisomers is the main challenge for synthesizing the corresponding regioisomeric carborane products via metal-catalyzed cross-coupling. The two strategies are reminiscent of methods used for the functionalization of aromatic and heteroaromatic hydrocarbon

Special Issue: Honoring 25 Years of the Buchwald–Hartwig Amination

Received: June 6, 2019

Published: August 5, 2019

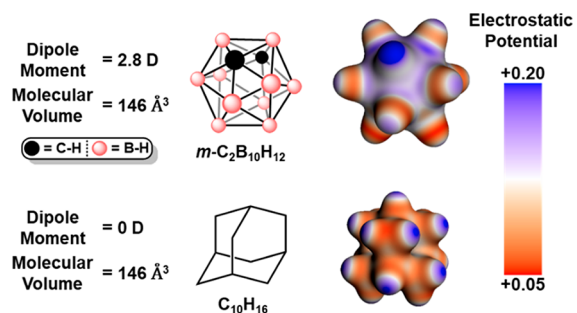


Figure 1. Electrostatic potential maps of *m*-carborane and adamantane and molecular volumes based on the Connolly solvent-excluded volume using a 1.4 Å probe sphere (see the [Supporting Information](#) for computational details).

congeners and are complementary in their nature. However, despite the prevalence of metal-catalyzed isomerization chemistry for hydrocarbon molecules, the methodology for accessing all four boron-substituted regioisomers for icosahedral carboranes is still fundamentally underexplored.

In the case of *m*-carborane (**mCB**), facile electrophilic halogenation occurs at the electron-rich B(9)–H vertex to produce 9-Br-*m*-carborane (**Br-B(9)**). However, synthesis of the other regioisomers (5-Br-*m*-carborane, **Br-B(5)**; 4-Br-*m*-carborane, **Br-B(4)**; and 2-Br-*m*-carborane, **Br-B(2)**) is more challenging. For example, deboronation and halogenation followed by boron vertex reinsertion enable the synthesis of some non-B(9)-vertex halogenated regioisomers.^{39,40} Alternatively, thermal isomerization of **Br-B(9)** occurs at temperatures >300 °C and produces a statistical distribution of 9/5/4/2-bromo-*m*-carborane (**Br-mCB**) isomers.^{41–44} The thermal isomerization process is one of the few methods to synthesize **Br-B(5)** and **Br-B(4)**. The difficulty associated with synthesizing these **mCB** regioisomers is perceived as a significant

obstacle to the study of carborane-based molecules and their regioisomers.

We recently reported the discovery of an off-cycle **Br-mCB** isomerization process (“cage-walking”) that bypasses the need to synthesize the B(9/5/4/2) **Br-mCB** regioisomers for subsequent cross-coupling to form B(9/5/4/2)-functionalized **mCB** regioisomers.⁴⁵ The cage-walking process isomerizes the **Br-B(9)** substrate into all four **Br-mCB** regioisomers ([Figure 2](#)). This tandem cage-walking/cross-coupling process allows **Br-B(9)** to serve as a precursor to B(9/5/4/2)-substituted **mCB**. The selectivity for cross-coupling at the B(5), B(4), and B(2) vertices appears to be driven by the increased electrophilicity of the Pd(II) center when the carborane is bound through the more electron-poor (B(2) > B(4) > B(5)) boron vertices.⁴⁵ However, to date the utility of the tandem cage-walking/cross-coupling process has been limited to sterically hindered nucleophiles. Thus, we set out to (1) understand the reaction conditions necessary to access the cage-walking process and (2) identify methods for controlling the cross-coupling of sterically unencumbered nucleophiles.

RESULTS AND DISCUSSION

Cage-Walking Isomerization by [LPd]. In order to integrate the cage-walking process into various Pd-catalyzed cross-coupling reactions, we set out to identify the reaction components that facilitate Pd-catalyzed **Br-B(9)** isomerization. In our previous studies we used an [XPhos-Pd-G3] precatalyst to generate the active [XPhosPd] catalytic species.⁴⁵ This method required the use of an exogenous base to deprotonate the precatalyst, which produced [XPhosPd] by reductive elimination of a carbazole molecule.⁴⁶ To evaluate whether cage-walking occurs in the absence of precatalyst byproducts, we prepared the [XPhosPd] catalyst by using [Pd(cod)-(CH₂Si(CH₃)₃)₂] (cod = 1,5-cyclooctadiene) as an alternative

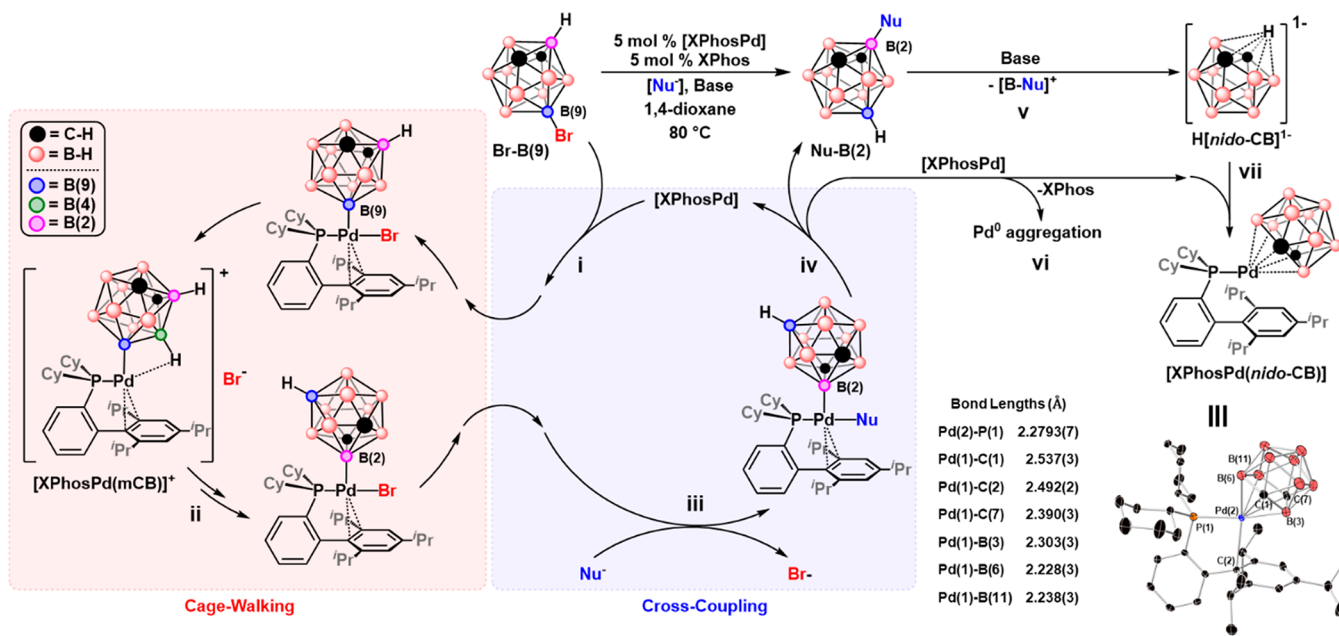


Figure 2. Proposed tandem cage-walking/cross-coupling cycle. The red box encapsulates the cage-walking process, and the blue box encapsulates the cross-coupling process. Deleterious off-cycle pathways are shown on the right side of the tandem cage-walking/cross-coupling, and the inset shows the single-crystal X-ray diffraction crystal structure of [XPhosPd(*nido*-CB)]. Steps: (i) oxidative addition; (ii) cage-walking; (iii) transmetalation; (iv) reductive elimination; (v) deboronation of Nu-B(2) by base; (vi) aggregation of palladium into palladium particles; (vii) ligation of [XPhosPd] by *nido*-CB.

Pd⁰ source in the presence of dialkylbiarylphosphine ligands.⁴⁷ Similar to the [XPhos-Pd-G3] precatalyst system, we observed cage-walking when Br-B(9) was treated with a solution of [XPhosPd] at 80 °C (Figure 3), suggesting that the cage-

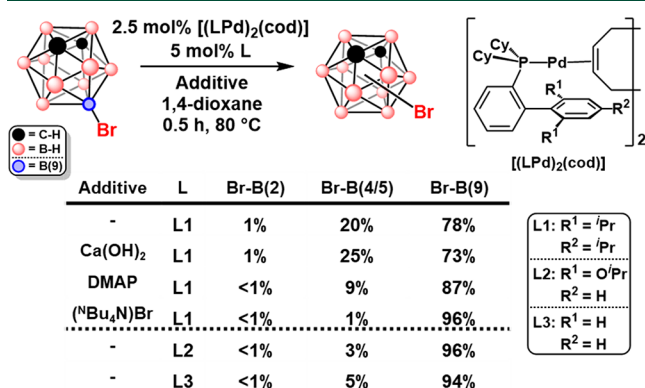


Figure 3. GC–MS yields of Br-*m*CB regioisomers produced by Pd-catalyzed cage-walking starting with Br-B(9).

walking process is independent of the presence of the base and likely proceeds via unimolecular isomerization. Since there is no oxidant in the reaction mixture strong enough to facilitate a Pd(II)/Pd(IV) cycle, we believe that the cage-walking process likely does not involve a Pd(IV) intermediate (see Figure S12 for proposed cage-walking mechanisms). Examination of other dialkylbiarylphosphine ligands (RuPhos, L2; CyJohnPhos, L3) revealed that the cage-walking process is not exclusive to the XPhos ligand. However, the total isomer yield is highest when XPhos (L1) is used. Notably, we did not observe cage-walking isomerization of 9-*I*-*m*-carborane in the presence of 5 mol % [XPhos-Pd-G3] precatalyst with K₃PO₄ in 1,4-dioxane at 80 °C.

Next, we examined whether certain additives could affect the amounts of Br-*m*CB isomers formed during cage-walking (Figure 3). We found that presence of Lewis bases or excess bromide reduces the relative ratios of cage-walked Br-*m*CB isomers. For example, addition of 4-dimethylaminopyridine (DMAP) or (ⁿBu₄N)Br reduced the yield of B(2/4/5) Br-*m*CB isomers from 21% to 10% and 1%, respectively. These observations would be consistent with a catalytically relevant ([XPhosPd(*m*CB)]⁺) intermediate for the cage-walking process in which the formally cationic Pd center bears a vacant coordination site (Figures 2 and S12). In order to probe this mechanistic hypothesis further, we focused on additives that might promote Pd–Br bond cleavage in [XPhosPd(*m*CB)Br] to yield an [XPhosPd(*m*CB)]⁺ species with a vacant coordination site that we suspect is responsible for the activation of an adjacent B–H bond and subsequent cage-walking. Importantly, the total yield of B(2/4/5) Br-*m*CB isomers can be increased from 20% to 26% by addition of Ca(OH)₂ to the cage-walking reaction. This increase in the yield of Br-*m*CB isomers is attributed to the ability of layered hydroxides to intercalate anions and form OH⋯Br interactions that may promote the formation of [XPhosPd(*m*CB)]⁺.⁴⁸ We also found that the identity of the base (including those soluble in organic media, e.g., triethylamine) had little effect on Br-B(9) isomerization, and only 1 equiv of base (relative to [XPhos-Pd-G3] precatalyst) was needed to form the [XPhosPd] complex. This set of experiments demonstrates how certain additives or reaction byproducts can affect the

cage-walking process and the overall distribution of *m*CB regioisomers.

Tandem Cage-Walking/Suzuki–Miyaura Coupling. In our initial study of tandem cage-walking/cross-coupling with phenols, we observed that the combination of a sterically encumbered biarylphosphine ligand and a sterically encumbered substrate generate a higher percentage of B(2) regioisomers than their less hindered counterparts.⁴⁵ For example, under otherwise identical conditions, tandem cage-walking/cross-coupling of 3,5-dimethylphenol with Br-B(9) gave a 30% yield of B(2)-substituted *m*CB, whereas the bulkier but electronically comparable 2,6-trimethylphenol gave a 76% yield of B(2)-substituted *m*CB.⁴⁵ This pronounced selectivity for cage-walking was attributed to the substrate control engendered by the sterics of the phenol moiety that can modulate the rate of transmetalation. We hypothesized that such steric control may not be necessary in the case of other substrates such as arylboronic acids, where the electronic properties of the aryl substituent can dictate the rate of transmetalation. For example, the tandem cage-walking/Suzuki–Miyaura coupling of *p*-tolylboronic acid with Br-B(9) produced the *p*-tolyl-B(2) isomer as the major product.⁴⁵ This suggests that certain transmetalating agents can mitigate the nucleophilicity of the cross-coupling partner and allow the relative rates of cage-walking and transmetalation to be competitive with each other.

We surveyed the steric and electronic effects of –F and –OCH₃ substituents on the efficacy of tandem cage-walking/Suzuki–Miyaura cross-coupling. Generally, we found that electron-rich arylboronic acids (*p*/*m*/*o*-methoxyphenylboronic acid) produced more *B*-aryl-*m*-carborane (Aryl-*m*CB) than electron-poor arylboronic acids (*p*/*m*/*o*-fluorophenylboronic acid) (Figure 4). The presence of an ortho substituent appears

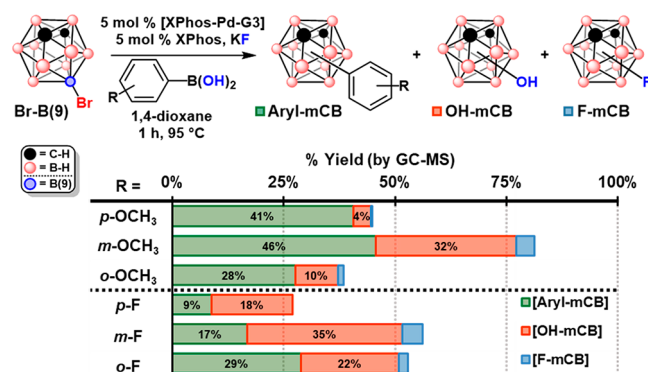


Figure 4. GC–MS yields of carborane-containing species produced during tandem cage-walking/Suzuki–Miyaura cross-coupling.

to have an inhibitory effect on the cross-coupling of *o*-methoxyphenylboronic acid but has a beneficial effect for *o*-fluorophenylboronic acid. Although both functional groups are ortho-directing, the increased steric bulk of the –OCH₃ group near the nucleophilic site may inhibit transmetalation and lead to less Aryl-*m*CB formation. Conversely, electron-poor arylboronic acids resulted in lower Aryl-*m*CB yields and more byproduct formation (vide infra). These differences in Aryl-*m*CB yield may be due to the reduced nucleophilicity of the aryl moiety more difficult. Additionally, arylboronic acids bearing Lewis basic groups such as 4-cyanophenylboronic acid

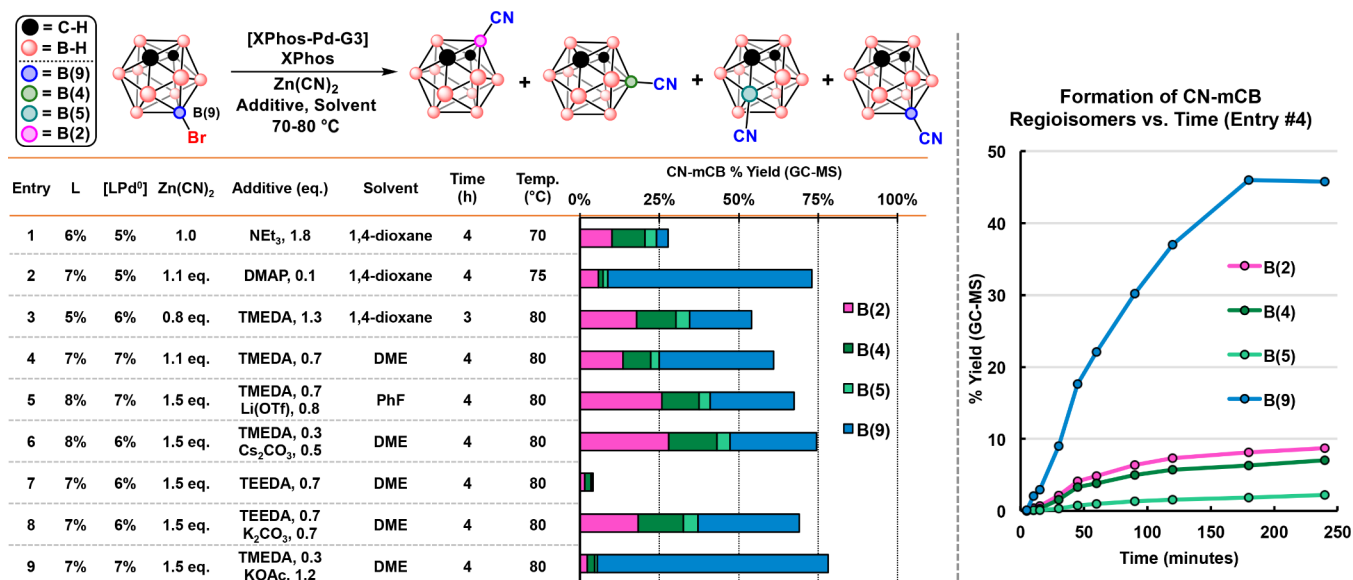


Figure 5. (left) Optimization of the tandem cage-walking/cross-coupling cyanation reaction. The bar graph indicates GC–MS yields of the cyano-*m*-carborane regioisomers for each reaction entry. (right) GC–MS reaction monitoring of cyano-*m*-carborane (CN-*m*CB) regioisomers produced during tandem cage-walking/cross-coupling.

and 3-pyridylboronic acid did not result in cross-coupling. The presence of Lewis basic groups in 4-cyanophenylboronic acid and 3-pyridylboronic acid can suppress the cage-walking process, which may prevent the formation of the more electrophilic B(2)-bound [XPhosPd(*m*CB)]⁺ catalyst species.⁴⁹

In addition to the formation of Aryl-*m*CB, we also observed the formation of *B*-hydroxy-*m*-carborane regioisomers (OH-*m*CB) and *B*-fluoro-*m*-carborane (F-*m*CB) as a byproduct of the tandem cage-walking/cross-coupling (Figure 4). While the formation of OH-*m*CB was observed previously by us and others^{26,50} and is likely due to the presence of adventitious moisture in the system, the formation of F-*m*CB by cross-coupling of nucleophilic fluoride is rare.²⁷ Neither of these byproducts are surprising given the larger thermodynamic driving force for the formation of B–O and B–F bonds relative to C–O and C–F bonds.⁵¹ This contrasts with Suzuki–Miyaura cross-coupling reactions, where off-cycle C–O and C–F bond formation is rarely observed even under aqueous reaction conditions. Notably, arylboronic acids with electron-withdrawing groups resulted in more OH-*m*CB than electron-rich arylboronic acids. The formation of OH-*m*CB may be due to transmetalation of the hydroxyl group from the boronic acid or from OH-containing byproducts resulting from its decomposition.

During the isolation of the Aryl-*m*CB compounds, we identified an air- and chromatographically stable ruby-colored compound that formed as a byproduct of the Suzuki–Miyaura cross-coupling reactions. Chromatographic isolation followed by spectroscopic analysis (¹¹B, ¹H, and ³¹P NMR spectroscopy) suggested a species containing a metal-bound phosphine as well as a boron-cluster-containing fragment. Single-crystal X-ray crystallography of this material revealed a Pd-based complex containing an XPhos ligand bound in a κ²-*P,C* fashion. The coordination sphere of the Pd center is completed by a dicarbollide ligand ([*nido*-7,9-*C*₂B₉H₁₁]²⁻, *nido*-CB) bound in an η⁵ fashion. On the basis of the nature of the phosphine and *nido*-CB ligands, the formal oxidation state of the Pd center in [XPhosPd(*nido*-CB)] is +2. Deboronation of

carboranes is known to occur by nucleophilic attack at the electron-poor boron vertices of carboranes (Figure 2, step v).^{52–54} Small nucleophiles such as F[−] and OH[−] can cause deboronation of R-*m*CB in situ to form the η⁵-[*nido*-7,9-*C*₂B₉H₁₂][−] ligand, which after deprotonation binds to the [XPhosPd] complex (vide infra).^{52,53,55} To probe this pathway further, an independent synthesis of the [XPhosPd(*nido*-CB)] complex was accomplished by the reaction of (ⁿBu₄N)[*nido*-7,9-*C*₂B₉H₁₂] with the [XPhos-Pd-G3] precatalyst. We found that [XPhosPd(*nido*-CB)] is not an active catalyst in carborane cross-coupling reactions, likely because of the greater coordinative saturation of the Pd center by the *nido*-CB ligand and the inability to regenerate Pd⁰ from this species under the reaction conditions.^{56–58}

A unique aspect of [XPhosPd(*nido*-CB)] is the lack of an exohedral functional group on the *nido*-CB ligand despite the use of functionalized carborane substrates. This suggests that cage-walking to the B(2) vertex may also activate the carborane toward deboronation and lead to deactivation of the [XPhosPd] catalyst by the formation of [XPhosPd(*nido*-CB)] (Figure 2, step vii). One possible decomposition route may be cage-walking/cross-coupling of OH[−] or F[−] at the B(2) vertex to generate a B(2)-X'-carborane (X' = OH, F) that is more easily deboronated than B(2)-R-carborane (R = H, aryl).^{52–55,59–61} Previous studies of carborane deboronation indicate that coordination of several nucleophiles to a B–H vertex is necessary to remove a boron vertex from the carborane cage.^{54,59,60} Thus, off-cycle coupling of a small nucleophile such as OH[−] or F[−] at B(2) may activate the B(2)-X'-carborane (X' = OH, F) toward deboronation and formation of *nido*-CB. This highlights the intricacies of using carborane substrates in cross-coupling, particularly in the presence of small nucleophiles, which can turn a substrate into a catalyst poison. Importantly, this mode of decomposition is distinctly different from the classical cross-coupling chemistry of aryl-based species and necessitates high Pd catalyst loadings.

Tandem Cage-Walking/Cyanation. Our studies of Br-*m*CB isomerization and tandem cage-walking/Suzuki–Miyaura coupling have so far revealed that tandem cage-

walking/cross-coupling is possible with sterically unencumbered nucleophiles. With these observations in mind, we set out to integrate the cage-walking cycle into Pd-catalyzed cross-coupling of a small nucleophile (CN^-). If successful, the resulting cyano-*m*-carborane (**CN-mCB**) regioisomers can be useful synthons in materials and medicinal chemistry.^{30,62,63}

Cross-coupling of cyanide is a challenging transformation in general because of the strong affinity of the CN^- ligand to Pd(II), which leads to the formation of catalytically inactive species.⁶⁴ Efforts to prevent catalyst poisoning have previously focused on reducing and constantly maintaining a small amount of CN^- in the reaction mixture.⁶⁵ For our transformation, we chose $\text{Zn}(\text{CN})_2$ as a cyanide source and transmetalation agent because of its strong CN^- binding affinity to Zn(II), which prevents the formation of free CN^- at high $\text{Zn}(\text{CN})_2$ concentrations. Additionally, the redox non-activity and weak binding of phosphine ligands to Zn(II) decreases the likelihood of [XPhosPd] oxidation or phosphine sequestration.⁶⁶

Although $\text{Zn}(\text{CN})_2$ is insoluble in most organic solvents because of the bridging μ^2 coordination of CN^- across zinc centers, forming Zn-CN-Zn-based coordination polymers in the solid state,⁶⁷ $\text{Zn}(\text{CN})_2$ can be solubilized in alkaline and ammoniacal environments.^{68–73} However, alkaline conditions may lead to undesirable **OH-mCB** formation or deboration, as observed with the Suzuki–Miyaura cross-coupling reactions (vide supra). Alternatively, trialkylamines are suitable ligands for $\text{Zn}(\text{CN})_2$ because they do not inhibit **Br-mCB** cage-walking, do not readily participate in the cross-coupling reaction, and can partially solubilize $\text{Zn}(\text{CN})_2$.^{68,71} Initially we used NEt_3 as a base to activate the [XPhos-Pd-G3] precatalyst and solubilize $\text{Zn}(\text{CN})_2$, which led to a modest yield (<30% by GC–MS) of **CN-mCB** isomers (Figure 5, entry 1). Importantly, despite the low yield of **CN-mCB**, the **CN-B(2)** and **CN-B(4)** regioisomers were produced as the major **CN-mCB** products, validating our original hypothesis that under well-designed conditions small nucleophiles can be competent substrates in the discovered cage-walking process.

We then explored whether bidentate alkylamine ligands could increase the yield of **CN-mCB** by increasing the solubility of $\text{Zn}(\text{CN})_2$ and promoting transmetalation of the CN^- anion from Zn to Pd. Use of *N,N,N',N'*-tetramethylethylenediamine (TMEDA) as a ligand for $\text{Zn}(\text{CN})_2$ increased the overall yield of **CN-mCB** regioisomers (65% by GC–MS), but the improvement in the **CN-mCB** yield also increased the amount of **CN-B(9)** relative to the B(2/4/5) **CN-mCB** regioisomers (Figure 5, entry 3). Switching to a larger bidentate alkylamine ligand, *N,N,N',N'*-tetraethylethylenediamine (TEEDA), significantly decreased the amount of **CN-B(9)** relative to the B(2/4/5) **CN-mCB** regioisomers (Figure 5, entry 7), but it also decreased the overall **CN-mCB** yield (<5% by GC–MS). This shows that increasing the steric bulk of the transmetalating agent to promote tandem cage-walking/cross-coupling can have deleterious effects on the overall cross-coupling efficiency. In addition to using alkylamines, we also examined whether a N-donor heterocycle could increase the **CN-mCB** yield by increasing the solubility of $\text{Zn}(\text{CN})_2$. The use of 4-(*N,N*-dimethylamino)pyridine (DMAP) as a ligand for $\text{Zn}(\text{CN})_2$ significantly increased the yield of **CN-mCB** (74% by GC–MS), but the isomer distribution was mostly **CN-B(9)** (Figure 5, entry 2). We attribute this difference in regioisomer distribution to suppression of the cage-walking pathway through reversible coordination of DMAP to

$[\text{XPhosPd}(\text{mCB})]^+$ and the increased lability of CN^- when $\text{Zn}(\text{CN})_2$ is ligated by the stronger N-donor DMAP ligand.

Despite improvements in the overall yield of **CN-mCB** regioisomers, we were unable to obtain complete conversion of **Br-B(9)** into **CN-mCB** regioisomers. As the tandem cage-walking/cross-coupling reaction proceeded, we observed darkening of the reaction mixture until a black/gray slurry formed within the first hour of the reaction. GC–MS analysis of a model cage-walking/cyanation reaction showed a gradual decay in the conversion of **Br-mCB** to **CN-mCB** until the reaction progress plateaued after ~3 h (Figure 5). This suggests that the incomplete conversion of **Br-mCB** to **CN-mCB** is partially due to Pd^0 aggregation to form black Pd^0 particles, which are not effective catalysts for carborane cross-coupling (Figure 2, step vi).

Suspecting that accumulation of Br^- may inhibit further conversion of **Br-mCB** to **CN-mCB**, we examined whether addition of alkali metal salts could improve the **CN-mCB** yield by sequestering Br^- . Addition of Cs_2CO_3 or $\text{Li}(\text{OTf})$ increased the overall yield of **CN-mCB** regioisomers without inhibiting the cage-walking process, whereas KOAc had an opposite effect that predominantly produced **CN-B(9)** (Figure 5, entry 9). The differences in regioisomer yield with different alkali metal salts and N-donor ligands may be due to the speciation of $\text{Zn}(\text{CN})_2$ into mono-, di-, tri-, and tetracyanozincate species.^{71,74–76} The formation of various zinc cyanide species due to ligation by additives and reaction byproducts may alter the rate of CN^- transmetalation and account for the various **CN-mCB** regioisomer distributions observed throughout this study. Overall, through our optimization studies we developed several conditions to selectively control the incorporation of the cage-walking process into catalytic cross-coupling with small nucleophiles. In particular, if deactivation of the cage-walking process is desired, the addition of a Lewis base (e.g., DMAP; Figure 5, entry 2) effectively favors B(9) coupling. Alternatively, if the cage-walking process is desired, care should be taken to reduce the amount of Lewis basic species (e.g., Brønsted base or halide counterion) that can bind the proposed $[\text{XPhosPd}(\text{mCB})]^+$ intermediate that leads to isomerization of **Br-mCB**.

CONCLUSIONS

Off-cycle processes in carborane cross-coupling were examined for their role in affecting tandem cage-walking/cross-coupling and in suppressing catalyst activity. The cage-walking process was studied in the absence and presence of a cross-coupling partner to identify conditions leading to tandem cage-walking/cross-coupling. We found that Pd-catalyzed cage-walking occurs with several dialkylbiarylphosphine ligands and that the cage-walking process can be enhanced or suppressed by the presence of additives such as $\text{Ca}(\text{OH})_2$ or DMAP, respectively. These insights allowed us to identify substrate transmetalation strategies for tandem cage-walking/cross-coupling reactions with sterically unencumbered nucleophiles such as arylboronic acids and cyanide. The results reported here demonstrate the feasibility of using sterically unencumbered substrates in tandem cage-walking/cross-coupling to synthesize B-substituted carborane regioisomers. These studies further highlight the importance of the bulky biaryl-based phosphine ligands originally developed by Buchwald and co-workers in transition metal catalysis by extending their application to organomimetic clusters.

■ ASSOCIATED CONTENT

S Supporting Information

The Supporting Information is available free of charge on the ACS Publications website at DOI: 10.1021/acs.oprd.9b00257.

Full procedures and crystallographic and other characterization data (PDF)

■ AUTHOR INFORMATION

Corresponding Author

*E-mail: spokoiny@chem.ucla.edu.

ORCID

Alexander M. Spokoiny: 0000-0002-5683-6240

Notes

The authors declare no competing financial interest.

■ ACKNOWLEDGMENTS

This article is dedicated to a mentor and friend, Professor Stephen L. Buchwald, whose seminal contributions to chemistry continue to inspire us all. We thank the NIGMS (R35GM124746) and the National Defense Science and Engineering Graduate Fellowship (NDSEG to R.M.D) for supporting this project.

■ REFERENCES

- (1) *Metal-Catalyzed Cross-Coupling Reactions*; de Meijere, A., Diederich, F., Eds.; Wiley-VCH: Weinheim, Germany, 2004.
- (2) Johansson Seechurn, C. C. C.; Kitching, M. O.; Colacot, T. J.; Snieckus, V. Palladium-Catalyzed Cross-Coupling: A Historical Contextual Perspective to the 2010 Nobel Prize. *Angew. Chem., Int. Ed.* **2012**, *51* (21), 5062–5085.
- (3) Shultz, L. H.; Brookhart, M. Measurement of the Barrier to β -Hydride Elimination in a β -Agostic Palladium–Ethyl Complex: A Model for the Energetics of Chain-Walking in (α -Diimine)PdR⁺ Olefin Polymerization Catalysts. *Organometallics* **2001**, *20* (19), 3975–3982.
- (4) Crabtree, R. H. Deactivation in Homogeneous Transition Metal Catalysis: Causes, Avoidance, and Cure. *Chem. Rev.* **2015**, *115* (1), 127–150.
- (5) Balcells, D.; Nova, A. Designing Pd and Ni Catalysts for Cross-Coupling Reactions by Minimizing Off-Cycle Species. *ACS Catal.* **2018**, *8* (4), 3499–3515.
- (6) Hassam, M.; Taher, A.; Arnott, G. E.; Green, I. R.; van Otterlo, W. A. L. Isomerization of Allylbenzenes. *Chem. Rev.* **2015**, *115* (11), 5462–5569.
- (7) Becica, J.; Glaze, O. D.; Wozniak, D. I.; Dobereiner, G. E. Selective Isomerization of Terminal Alkenes to (*Z*)-2-Alkenes Catalyzed by an Air-Stable Molybdenum(0) Complex. *Organometallics* **2018**, *37* (3), 482–490.
- (8) Milner, P. J.; Kinzel, T.; Zhang, Y.; Buchwald, S. L. Studying Regioisomer Formation in the Pd-Catalyzed Fluorination of Aryl Triflates by Deuterium Labeling. *J. Am. Chem. Soc.* **2014**, *136* (44), 15757–15766.
- (9) Li, J.; Sun, C.; Demerzhani, S.; Lee, D. Metal-Catalyzed Rearrangement of Cyclopropenes to Allenes. *J. Am. Chem. Soc.* **2011**, *133* (33), 12964–12967.
- (10) Curran, K.; Risse, W.; Hamill, M.; Saunders, P.; Muldoon, J.; Asensio De La Rosa, R.; Tritto, I. Palladium(II)-Catalyzed Rearrangement and Oligomerization Reactions of *cis*-Bicyclo[4.2.0]oct-7-ene. *Organometallics* **2012**, *31* (3), 882–889.
- (11) Wang, J. Y.; Strom, A. E.; Hartwig, J. F. Mechanistic Studies of Palladium-Catalyzed Aminocarbonylation of Aryl Chlorides with Carbon Monoxide and Ammonia. *J. Am. Chem. Soc.* **2018**, *140* (25), 7979–7993.
- (12) Hartwig, J. F. Catalyst-Controlled Site-Selective Bond Activation. *Acc. Chem. Res.* **2017**, *50* (3), 549–555.
- (13) Larsen, C. R.; Grotjahn, D. B. Stereoselective Alkene Isomerization over One Position. *J. Am. Chem. Soc.* **2012**, *134* (25), 10357–10360.
- (14) Lee, C. W.; Zhuang, Z. P.; Kung, M. P.; Plössl, K.; Skovronsky, D.; Gur, T.; Hou, C.; Trojanowski, J. Q.; Lee, V. M. Y.; Kung, H. F. Isomerization of (*Z,Z*) to (*E,E*)1-Bromo-2,5-bis-(3-hydroxycarbonyl-4-hydroxy)-styrylbenzene in Strong Base: Probes for Amyloid Plaques in the Brain. *J. Med. Chem.* **2001**, *44* (14), 2270–2275.
- (15) Li, J.; Logan, C. F.; Jones, M. Simple Syntheses and Alkylation Reactions of 3-Iodo-*o*-carborane and 9,12-Diiodo-*o*-carborane. *Inorg. Chem.* **1991**, *30* (25), 4866–4868.
- (16) Eriksson, L.; Beletskaya, I.; Bregadze, V.; Sivaev, I.; Sjöberg, S. Palladium-Catalyzed Cross-Coupling Reactions of Arylboronic Acids and 2-*I-p*-Carborane. *J. Organomet. Chem.* **2002**, *657* (1–2), 267–272.
- (17) Lin, F.; Yu, J.-L.; Shen, Y.; Zhang, S.-Q.; Spingler, B.; Liu, J.; Hong, X.; Duttwyler, S. Palladium-Catalyzed Selective Five-Fold Cascade Arylation of the 12-Vertex Monocarborane Anion by B–H Activation. *J. Am. Chem. Soc.* **2018**, *140* (42), 13798–13807.
- (18) Cheng, R.; Li, B.; Wu, J.; Zhang, J.; Qiu, Z.; Tang, W.; You, S. L.; Tang, Y.; Xie, Z. Enantioselective Synthesis of Chiral-at-Cage *o*-Carboranes via Pd-Catalyzed Asymmetric B–H Substitution. *J. Am. Chem. Soc.* **2018**, *140* (13), 4508–4511.
- (19) Anderson, K. P.; Mills, H. A.; Mao, C.; Kirlikovali, K. O.; Axtell, J. C.; Rheingold, A. L.; Spokoiny, A. M. Improved Synthesis of Icosahedral Carboranes Containing Exopolyhedral B–C and C–C Bonds. *Tetrahedron* **2019**, *75* (2), 187–191.
- (20) Beletskaya, I. P.; Bregadze, V. I.; Ivushkin, V. A.; Zhigareva, G. G.; Petrovskii, P. V.; Sivaev, I. B. Palladium-Catalyzed Alkynylation of 2-Iodo-*p*-carboranes and 9-Iodo-*m*-carboranes. *Russ. J. Org. Chem.* **2005**, *41* (9), 1359–1366.
- (21) Sevryugina, Y.; Julius, R. L.; Hawthorne, M. F. Novel Approach to Aminocarboranes by Mild Amidation of Selected Iodo-Carboranes. *Inorg. Chem.* **2010**, *49* (22), 10627–10634.
- (22) Kabytaev, K. Z.; Everett, T. A.; Safronov, A. V.; Sevryugina, Y. V.; Jalisatgi, S. S.; Hawthorne, M. F. B-Mercaptocarboranes: A New Synthetic Route. *Eur. J. Inorg. Chem.* **2013**, *2013* (14), 2488–2491.
- (23) Safronov, A. V.; Kabytaev, K. Z.; Jalisatgi, S. S.; Hawthorne, M. F. Novel Iodinated Carboranes: Synthesis of the 8-Iodo-7,9-dicarbonyl-undecaborate Anion and 2-Iodo-1,7-dicarbonyl-dodecaborane. *Dalton Trans.* **2014**, *43* (33), 12467.
- (24) Wingen, L. M.; Scholz, M. S. B-Cyanodicarba-*closo*-dodecaboranes: Facile Synthesis and Spectroscopic Features. *Inorg. Chem.* **2016**, *55* (17), 8274–8276.
- (25) Saleh, L. M. A.; Dziedzic, R. M.; Khan, S. I.; Spokoiny, A. M. Forging Unsupported Metal–Boryl Bonds with Icosahedral Carboranes. *Chem. - Eur. J.* **2016**, *22* (25), 8466–8470.
- (26) Dziedzic, R. M.; Saleh, L. M. A.; Axtell, J. C.; Martin, J. L.; Stevens, S. L.; Royappa, A. T.; Rheingold, A. L.; Spokoiny, A. M. B–N, B–O, and B–CN Bond Formation via Palladium-Catalyzed Cross-Coupling of B-Bromo-Carboranes. *J. Am. Chem. Soc.* **2016**, *138* (29), 9081–9084.
- (27) Ishita, K.; Khalil, A.; Tiwari, R.; Gallucci, J.; Tjarks, W. Bis(*tert*-butylphosphine)palladium(0)-Catalyzed Iodine–Fluorine Exchange at *closo*-Carboranes. *Eur. J. Inorg. Chem.* **2018**, *2018* (24), 2821–2825.
- (28) Leites, L. A.; Introduction, I.; Boranes, I.; Boranes, I.; Modes, B.; Boranes, G. I.; Heteroatoms, C. Vibrational Spectroscopy of Carboranes and Parent Boranes and Its Capabilities in Carborane Chemistry. *Chem. Rev.* **1992**, *92* (2), 279–323.
- (29) Bendel, P. Biomedical Applications of ¹⁰B and ¹¹B NMR. *NMR Biomed.* **2005**, *18* (2), 74–82.
- (30) Leśnikowski, Z. J. Challenges and Opportunities for the Application of Boron Clusters in Drug Design. *J. Med. Chem.* **2016**, *59* (17), 7738–7758.
- (31) Messina, M. S.; Graefe, C. T.; Chong, P.; Ebrahim, O. M.; Pathuri, R. S.; Bernier, N. A.; Mills, H. A.; Rheingold, A. L.; Frontiera, R. R.; Maynard, H. D.; Spokoiny, A. M. Carborane RAFT Agents as

Tunable and Functional Molecular Probes for Polymer Materials. *Polym. Chem.* **2019**, *10* (13), 1660–1667.

(32) Serino, A. C.; Anderson, M. E.; Saleh, L. M. A.; Dziedzic, R. M.; Mills, H.; Heidenreich, L. K.; Spokoyny, A. M.; Weiss, P. S. Work Function Control of Germanium through Carborane-Carboxylic Acid Surface Passivation. *ACS Appl. Mater. Interfaces* **2017**, *9* (40), 34592–34596.

(33) Quan, Y.; Qiu, Z.; Xie, Z. Transition-Metal-Catalyzed Selective Cage B–H Functionalization of *o*-Carboranes. *Chem. - Eur. J.* **2018**, *24* (12), 2795–2805.

(34) Duttwyler, S. Recent Advances in B–H Functionalization of Icosahedral Carboranes and Boranes by Transition Metal Catalysis. *Pure Appl. Chem.* **2018**, *90* (4), 733–744.

(35) Quan, Y.; Xie, Z. Controlled Functionalization of *o*-Carborane via Transition Metal Catalyzed B–H Activation. *Chem. Soc. Rev.* **2019**, *48*, 3660–3673.

(36) Lyu, H.; Zhang, J.; Yang, J.; Quan, Y.; Xie, Z. Catalytic Regioselective Cage B(8)–H Arylation of *o*-Carboranes via “Cage-Walking” Strategy. *J. Am. Chem. Soc.* **2019**, *141* (10), 4219–4224.

(37) Eleazer, B. J.; Smith, M. D.; Popov, A. A.; Peryshkov, D. V. Expansion of the (BB)₂Ru Metallacycle with Coinage Metal Cations: Formation of B–M–Ru–B (M = Cu, Ag, Au) Dimetalacyclodiborolys. *Chem. Sci.* **2018**, *9* (9), 2601–2608.

(38) Dziedzic, R. M.; Spokoyny, A. M. Metal-Catalyzed Cross-Coupling Chemistry with Polyhedral Boranes. *Chem. Commun.* **2019**, *55* (4), 430–442.

(39) Safronov, A. V.; Sevryugina, Y. V.; Jalisatgi, S. S.; Kennedy, R. D.; Barnes, C. L.; Hawthorne, M. F. Unfairly Forgotten Member of the Iodocarborane Family: Synthesis and Structural Characterization of 8-Iodo-1,2-dicarba-*closo*-dodecaborane, Its Precursors, and Derivatives. *Inorg. Chem.* **2012**, *51* (4), 2629–2637.

(40) Safronov, A. V.; Kabytaev, K. Z.; Jalisatgi, S. S.; Hawthorne, M. F. Novel Iodinated Carboranes: Synthesis of the 8-Iodo-7,9-dicarba-*nido*-undecaborate anion and 2-Iodo-1,7-dicarba-*closo*-dodecaborane. *Dalton Trans.* **2014**, *43* (33), 12467–12469.

(41) Lipscomb, W. N. Framework Rearrangement in Boranes and Carboranes. *Science* **1966**, *153* (3734), 373–378.

(42) Kalinin, V. N.; Kobel'kova, N. I.; Zakharkin, L. I. Synthesis of 2- and 4-Aryl-*m*-Carboranes and Electronic Effects of the 4-*m*-Carboranyl Group. *J. Organomet. Chem.* **1979**, *172* (4), 391–395.

(43) Baše, T.; Macháček, J.; Hájková, Z.; Langecker, J.; Kennedy, J. D.; Carr, M. J. Thermal Isomerizations of Monothiolated Carboranes (HS)₂C₂B₁₀H₁₁ and the Solid-State Investigation of 9-(HS)-1,2-C₂B₁₀H₁₁ and 9-(HS)-1,7-C₂B₁₀H₁₁. *J. Organomet. Chem.* **2015**, *798*, 132–140.

(44) Bakardjiev, M.; Štíbr, B.; Holub, J.; Padělková, Z.; Růžička, A. Simple Synthesis, Halogenation, and Rearrangement of *closo*-1,6-C₂B₈H₁₀. *Organometallics* **2015**, *34* (2), 450–454.

(45) Dziedzic, R. M.; Martin, J. L.; Axtell, J. C.; Saleh, L. M. A.; Ong, T. C.; Yang, Y. F.; Messina, M. S.; Rheingold, A. L.; Houk, K. N.; Spokoyny, A. M. Cage-Walking: Vertex Differentiation by Palladium-Catalyzed Isomerization of B(9)-Bromo-*meta*-Carborane. *J. Am. Chem. Soc.* **2017**, *139* (23), 7729–7732.

(46) Bruno, N. C.; Tudge, M. T.; Buchwald, S. L. Design and Preparation of New Palladium Precatalysts for C–C and C–N Cross-Coupling Reactions. *Chem. Sci.* **2013**, *4* (3), 916–920.

(47) Lee, H. G.; Milner, P. J.; Buchwald, S. L. An Improved Catalyst System for the Pd-Catalyzed Fluorination of (Hetero)aryl Triflates. *Org. Lett.* **2013**, *15* (21), 5602–5605.

(48) Rajamathi, M.; Vishnu Kamath, P.; Seshadri, R. Polymorphism in Nickel Hydroxide: Role of Interstratification. *J. Mater. Chem.* **2000**, *10* (2), 503–506.

(49) Düfert, M. A.; Billingsley, K. L.; Buchwald, S. L. Suzuki–Miyaura Cross-Coupling of Unprotected, Nitrogen-Rich Heterocycles: Substrate Scope and Mechanistic Investigation. *J. Am. Chem. Soc.* **2013**, *135* (34), 12877–12885.

(50) Beletskaya, I. P.; Bregadze, V. I.; Kabytaev, K. Z.; Zhigareva, G. G.; Petrovskii, P. V.; Glukhov, I. V.; Starikova, Z. A. Palladium-

Catalyzed Amination of 2-Iodo-*para*-Carborane. *Organometallics* **2007**, *26* (9), 2340–2347.

(51) Darwent, B. deB. *Bond Dissociation Energies in Simple Molecules*; National Standard Reference Data Series, National Bureau of Standards, Vol. 31; U.S. National Bureau of Standards: Gaithersburg, MD, 1970; p 48.

(52) Fox, M. A.; Gill, W. R.; Herbertson, P. L.; MacBride, J. A. H.; Wade, K.; Colquhoun, H. M. Deboronation of C-Substituted *ortho*- and *meta*-*closo*-Carboranes Using “Wet” Fluoride Ion Solutions. *Polyhedron* **1996**, *15* (4), 565–571.

(53) Fox, M. A.; Wade, K. Deboronation of 9-Substituted-*ortho*- and -*meta*-Carboranes. *J. Organomet. Chem.* **1999**, *573* (1–2), 279–291.

(54) Taoda, Y.; Sawabe, T.; Endo, Y.; Yamaguchi, K.; Fujii, S.; Kagechika, H. Identification of an Intermediate in the Deboronation of *ortho*-Carborane: An Adduct of *ortho*-Carborane with Two Nucleophiles on One Boron Atom. *Chem. Commun.* **2008**, No. 17, 2049–2051.

(55) Yoo, J.; Hwang, J. W.; Do, Y. Facile and Mild Deboronation of *o*-Carboranes Using Cesium Fluoride. *Inorg. Chem.* **2001**, *40* (3), 568–570.

(56) Warren Jr, L.; Hawthorne, M. Metallocene Analogs of Copper, Gold, and Palladium Derived from the (3)-1,2-Dicarbollide Ion. *J. Am. Chem. Soc.* **1968**, *90* (18), 4823–4828.

(57) Jasper, S. A.; Huffman, J. C.; Todd, L. J. Palladium-Assisted Cyano Substitution Reactions of (PMe₂Ph)₂Pd(B₉H₉As₂) and (PMe₂Ph)₂Pd(B₉C₂H₁₁). X-ray Crystal and Molecular Structures of 5-CN-1,1-(PMe₂Ph)₂-*closo*-1,2,3-PdAs₂B₉H₈, 1-^tBuNC-5-CN-1-(PMe₂Ph)-*closo*-1,2,3-PdAs₂B₉H₈, and 4,5-(CN)₂-1,1-(PMe₂Ph)₂-*closo*-1,2,3-PdC₂B₉H₈. *Inorg. Chem.* **1995**, *34* (26), 6430–6439.

(58) Jasper, S. A.; Huffman, J. C.; Todd, L. J. Synthesis of a Metallaborane Complex Containing Pd(III) and the First Doubly Charge Compensated Ollide Ion. X-ray Crystal Structure of 1,4-Br₂-1,2,5-(PMe₂Ph)₃-*closo*-1-PdB₁₁H₈. *Inorg. Chem.* **1998**, *37* (23), 6060–6064.

(59) Willans, C. E.; Kilner, C. A.; Fox, M. A. Deboronation and Deprotonation of *ortho*-Carborane with N-Heterocyclic Carbenes. *Chem. - Eur. J.* **2010**, *16* (35), 10644–10648.

(60) Zheng, F.; Xie, Z. Reaction of *o*-Carboranes with Sterically Demanding N-Heterocyclic Carbene: Synthesis and Structural Characterization of 1:1 Adducts. *Dalton Trans.* **2012**, *41* (41), 12907–12914.

(61) Zhang, C. Y.; Cao, K.; Xu, T. T.; Wu, J.; Jiang, L.; Yang, J. A Facile Approach for the Synthesis of *Nido*-Carborane Fused Oxazoles via One Pot Deboronation/Cyclization of 9-Amide-*o*-Carboranes. *Chem. Commun.* **2019**, *55* (6), 830–833.

(62) Issa, F.; Kassiou, M.; Rendina, L. M. Boron in Drug Discovery: Carboranes as Unique Pharmacophores in Biologically Active Compounds. *Chem. Rev.* **2011**, *111* (9), 5701–5722.

(63) Scholz, M.; Hey-Hawkins, E. Carboranes as Pharmacophores: Properties, Synthesis, and Application Strategies. *Chem. Rev.* **2011**, *111* (11), 7035–7062.

(64) Erhardt, S.; Grushin, V. V.; Kilpatrick, A. H.; Macgregor, S. A.; Marshall, W. J.; Roe, D. C. Mechanisms of Catalyst Poisoning in Palladium-Catalyzed Cyanation of Haloarenes. Remarkably Facile C–N Bond Activation in the [(Ph³P)⁴Pd]/[Bu⁴N]⁺ CN-System. *J. Am. Chem. Soc.* **2008**, *130* (14), 4828–4845.

(65) Anbarasan, P.; Schareina, T.; Beller, M. Recent Developments and Perspectives in Palladium-Catalyzed Cyanation of Aryl Halides: Synthesis of Benzonitriles. *Chem. Soc. Rev.* **2011**, *40* (10), 5049–5067.

(66) Heaney, H. Zinc Cyanide. In *Encyclopedia of Reagents for Organic Synthesis*; John Wiley & Sons: Chichester, U.K., 2001; Vol. 3, p 533.

(67) Hoskins, B. F.; Robson, R. Design and Construction of a New Class of Scaffolding-like Materials Comprising Infinite Polymeric Frameworks of 3D-Linked Molecular Rods. A Reappraisal of the Zn(CN)₂ and Cd(CN)₂ Structures and the Synthesis and Structure of the Diamond-Related Framework. *J. Am. Chem. Soc.* **1990**, *112* (4), 1546–1554.

(68) Ahuja, I. S.; Singh, R. Bidentate Bridged Morpholine Complexes with Zinc(II) and Cadmium(II) Cyanides. *J. Coord. Chem.* **1976**, *5* (3), 167–170.

(69) Monge, A.; Martínez-Ripoll, M.; García-Blanco, S. The Adduct Zinc Dicyanide–Bis(2,9-Dimethyl-1,10-Phenanthroline) Trihydrate. *Acta Crystallogr., Sect. B: Struct. Crystallogr. Cryst. Chem.* **1978**, *34* (9), 2847–2850.

(70) Ho, K.; Yu, W.; Cheung, K.; Che, C. A Blue Photoluminescent $[Zn(L)(CN)_2]$ (L = 2,2'-Dipyridylamine) Material with a Supramolecular One-Dimensional Chain Structure. *Chem. Commun.* **1998**, *3* (19), 2101–2102.

(71) Jasiewicz, B.; Boczoń, W.; Mumot, A.; Warzajtis, B.; Rychlewska, U. Synthesis, Spectroscopy and Crystal Structure of α -Isparteine Complexes with ZnX^2 (X = Br, CN, Cl). *J. Mol. Struct.* **2005**, *737* (2–3), 239–244.

(72) Das, S.; Nag, A.; Goswami, D.; Bharadwaj, P. K. Zinc(II)- and Copper(I)-Mediated Large Two-Photon Absorption Cross Sections in a Bis-Cinnamaldiminato Schiff Base. *J. Am. Chem. Soc.* **2006**, *128* (2), 402–403.

(73) Sayin, E.; Kürkçüoğlu, G. S.; Yeşilel, O. Z.; Hökelek, T. Synthesis, Crystal Structure and Spectroscopic Properties of One-Dimensional Zinc(II)–Cyanide Complex with 1-Methylimidazole, $[Zn(\mu-CN)(CN)(1-meim)]_n$. *Z. Kristallogr. - Cryst. Mater.* **2015**, *230* (6), 421–426.

(74) Pickardt, J.; Staub, B. Kristallstruktur Des Cyanoverbrückten Polymeren Zinkcyanid-Pyridin-Komplexes $[Zn(Py)_2][Zn(CN)_4]^-$ / Crystal Structure of the Cyano Linked Polymeric Zinc Cyanide Pyridine Complex $[Zn(Py)_2][Zn(CN)_4]^-$. *Z. Naturforsch., B: J. Chem. Sci.* **1995**, *50* (10), 1517–1520.

(75) Guo, Y.; Weiss, R.; Boese, R.; Epple, M. Synthesis, Structural Characterization and Thermochemical Reactivity of Tris-(Ethylenediamine)Zinc Tetracyanozincate, a Precursor for Nanoscale ZnO. *Thermochim. Acta* **2006**, *446* (1–2), 101–105.

(76) Kürkçüoğlu, G. S.; Yeşilel, O. Z.; Şahin, O.; Sayin, E.; Büyükgüngör, O. Dinuclear Zinc(II) Complex with Tris(2-Aminoethyl) Amine Ligand: Synthesis, Structure and Properties. *Z. Kristallogr. - Cryst. Mater.* **2015**, *230* (6), 407–412.